Structural studies of annealed ultrathin $La_{0.8}MnO_3$ films

Q. Qian and T. A. Tyson[a)]
Department of Physics, New Jersey Institute of Technology, Newark, New Jersey 07102

C. Dubourdieu, A. Bossak, and J. P. Sénateur
Laboratoire des Matériaux et du Génie Physique, CNRS UMR 5628, ENSPG BP46, 38402 St. Martin d'Hères, France

M. Deleon
Department of Physics, New Jersey Institute of Technology, Newark, New Jersey 07102

J. Bai
Oak Ridge National Laboratory, Oak Ridge, Tennessee 37831

G. Bonfait
Nuclear and Technological Institute, Department of Chemistry, P-2686 Sacavem Codex, Portugal

(Received 26 November 2001; accepted for publication 28 February 2002)

A detailed study of the long-range, nanoscale, and local structure of $La_{0.8}MnO_3$ films of varying thickness was performed. These measurements give insight on the relative volumes of the insulating and metallic regions. A thin metallic surface region is found in all films. The nature of the film growth is also discussed. © *2002 American Institute of Physics.* [DOI: 10.1063/1.1470689]

Due to the large (colossal) magnetoresistance exhibited by perovskite manganites, they have attracted a great deal of interest for the potential applications.[1] It is evident that lattice strain plays an important role in the properties of these materials.[2,3] The first systematic experimental study of the effect of thickness on the magnetotransport properties of thin films was performed by Jin *et al.*[2] which was later followed by others.[3,4] The characteristic feature found is that the metal–insulator transition is suppressed in very thin films. Systematic magnetic studies have also been performed.[5–9] O'Donnel *et al.*[9] suggested that the magnetic anisotropy in films seen in many experiments is dominated by strain induced anisotropy leading to an easy axis which occurs parallel to or normal to the film plane depending on substrate induce compression or tension. The first attempt at quantifying the role of strain in these materials was made by Millis *et al.*[10] who showed that T_C is extremely sensitive to biaxial strain and that T_C reduction is quadratic in the Jahn–Teller distortion.[11] A bandstructure calculation of the phase diagram of tetragonal magnanites[12] showed that magnetic degrees of freedom can be indirectly controlled by lattice distortions via orbital degrees of freedom. It was argued that by changing the c/a ratio, the e_g orbital extending along the elongated Mn—O bond is preferentially occupied.

In unannealed thin films of $La_{0.7}Ca_{0.3}MnO_3$ (<250 Å) it is found the peak resistivity temperature T_p decreases with film thickness while the curie temperature T_C remains constant.[13] The difference between T_C and T_p is as large 100 K for a 50 Å films while the difference vanishes as in the case of bulk materials for films above 250 Å. Consistent with these results, other studies have shown that ultrathin films (~50 Å) become insulators.[3,4] In addition, it is found that annealing of thin films has a rather striking effect—it converts insulating ultrathin films into metallic films[3,14] and increases the Curie temperature and saturation magnetization of thick films.[3,15]

To understand the effect of thickness on the properties of ultrathin manganite films, we looked at three films (60, 300, and 1600 Å) of the ferromagnetic system $La_{0.8}MnO_3$. We examined the nanoscale structure by atomic force microscopy (AFM) measurements, the periodic structure by synchrotron x-ray diffraction (XRD) and the local atomic structure by near edge x-ray absorption spectroscopy. The AFM measurements reveal that the 60 Å film is composed of islands which coalesce into a smooth layer in the 300 Å film and lead to columnar growth in the 1600 Å film. A thin near surface region is found in all films by XRD. X-ray absorption measurements reveal significant local distortions occur in the MnO_6 octahedral of the 60 Å film (more distorted than $LaMnO_3$) while the differences between the 300 and 1600 Å films are small.

Epitaxial $La_{0.8}MnO_3$ films were grown on (001) $LaAlO_3$ substrates by metalorganic chemical vapor deposition using a liquid-injection source delivery system.[16,17] Deposition runs were carried out at 700 °C under a total pressure of 0.67 kPa and an oxygen partial pressure of 0.33 kPa. After deposition, films were *in situ* annealed at one atmosphere of oxygen at 800 °C for 15 min. Films of thicknesses 1600, 300, and 60 Å were prepared. The magnetization was measured in the range 4.2–320 K under a total magnetic field of 0.2 T in a vibrating sample magnetometer. The T_C values for the films were 180, 230, and 240 K for the 60 Å, 300 Å, and 1600 Å films, respectively. Resistivity measurements were performed using a four-point probe technique [see Fig. 2(c)]. The T_p (peak resistivity) values for the films were, 225 K, 255 K, and 260 K for the 60 Å, 300 Å, and 1600 Å films, respectively. All films were found to be metallic. A Digital Instruments AFM NanoScope IIIa operating in contact mode was used to investigate the surface morphology. Synchrotron XRD experiments were performed on the Oak Ridge National Laborato-

a)Electronic mail: tyson@adm.njit.edu

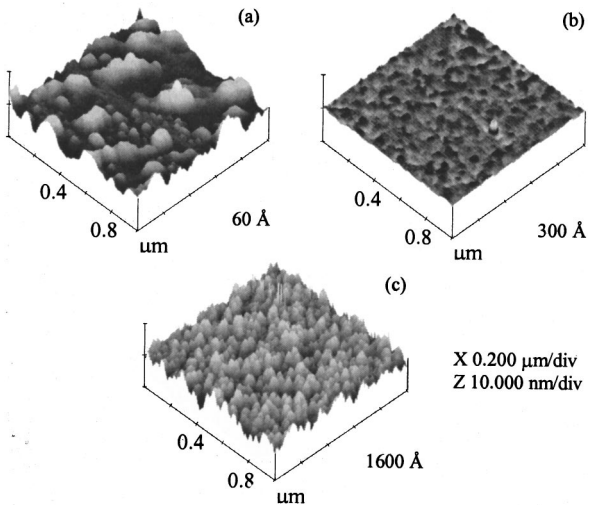

FIG. 1. AFM images of the 60 Å (a), 300 Å (b), and 1600 Å (c) films plotted on the same scale.

ry's X-ray beamline X14A at the National Synchrotron Light Source (NSLS) at the Brookhaven National Laboratory (BNL). The x-ray energy was set to 8.0468 keV ($\lambda = 1.5406$ Å). Mn *K*-edge absorption spectra in fluorescence mode were measured on NSLS beamline X19A. Measurements were made for films with the beam electric field polarization vector nearly 45° to the surface. The near edge spectra were area normalized.

In Fig. 1, we show the AFM images of the 60 Å (a), 300 Å (b), and 1600 Å (c) films plotted on the same scale. We can see that the 60 Å is not uniform but is composed of islands of $La_{0.8}MnO_3$. The islands become connected in the 300 Å film followed by columnar growth seen in the 1600 Å film. Interestingly, the 300 Å film is the most smooth film. Hence, as a function of thickness different growth mechanisms prevail. It may be expected that the island structure would result in insulating films. However, these annealed films are metallic [Fig. 2(c)]. As will be seen next, an unstrained surface region exists even in the thin films.

In Figs. 2(a) and 2(b), we show the diffraction profiles for two in-plane orthogonal reflections: (4 0 0) and (0 4 0). These measurements correspond to near 90° rotations relative to the (0 0 4) sample normal. We call these reflections in plane. For the 60 Å film, a pair of lines occurs at high angle relative to a pair lines found in the 1600 Å film at lower angle. While the corresponding pair of diffraction lines in the 300 Å film are significantly closer to those of the 1600 Å film than those of the 60 Å film. The 300 Å film has an additional peak (C_2) with *d* spacing similar to those of the 60 Å film. The substrate peak appears for all orientations at a higher angle indicating that the substrate has a smaller lattice constant than the films. From ϕ-scans, we find epitaxial growth in all of the films consistent with equal in-plane lattice parameters.

The two-peak structure is consistent with a film composed of two regions, one near the substrate (A peaks) which is highly constrained by the substrate lattice and a more relaxed region away from the substrate (B peaks) with significant lattice relaxation. Hence, the 300 and 1600 Å films are composed of a strained A layer with a relaxed B layer.

In the 60 Å film, the in-plane (400) and (040) reflections

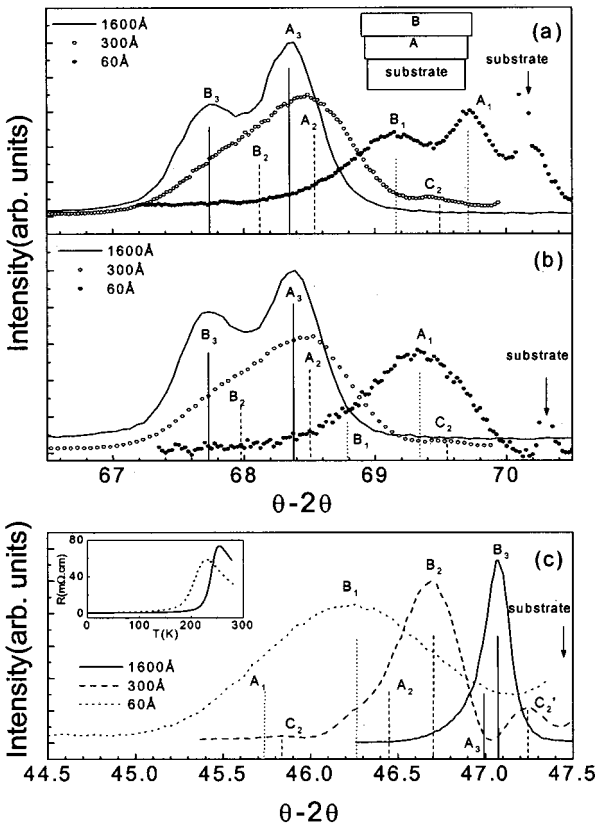

FIG. 2. XRD θ–2θ scans of $La_{0.8}MnO_3$ film with the scattering plane approximately parallel and normal to surface. Diffraction peaks for (a) measurements along the direction (4 0 0) and (b) along the direction (0 4 0) are shown as two in-plane scans. The out-of-plane (0 0 4) scan is given in (c). The solid line, open dotted line, and closed dotted lines are from the 1600 Å, 300 Å, 60 Å films, respectively. Each pattern was fit by a set of Gaussian peaks and the vertical bars show the approximate peak positions. The inset in (a) displays the two layer film model and the inset in (c) gives the resistivity curves of the 60 Å (dotted) and 1600 Å (solid) films.

yield A layer spacings of 1.347 Å and 1.353 Å, and B layer spacings of ~1.357 Å and 1.363 Å. That means that in the very thin film, there is in-plane asymmetry in both A and B layers. The 60 Å film tracks the substrate in-plane asymmetry as seen in the difference in the peak position for the substrate peaks. On the other hand, the 300 and 1600 Å films reveal no such asymmetry suggesting cubic symmetry.

In Fig. 2(c), we show the out-of-plane diffraction profiles for the three films. All profiles decomposed into ~two peaks except for the 300 Å films, which has at least four peaks with the addition of weak features labeled C_2 and C_2' at a low and high angle, respectively. Apart from these weaker peaks, the peaks positions (A and B) are quite consistent with the in-plane measurement if one assumes an approximately constant volume—if the film is compressed in plane, it will relax out of plane. In this way, the corresponding peak labels found in the in-plane measurements are matched to the out-of-plane measurements. The peak C_2' of the 300 Å film is possible corresponding to weak shoulder of in-plane scans.

From this discussion, we can see that strain in film is reduced as the thickness of the film increases and makes two different majority layers in films. At some critical thickness, for example 300 Å in this case, the strain produces some more very thin minority layers.

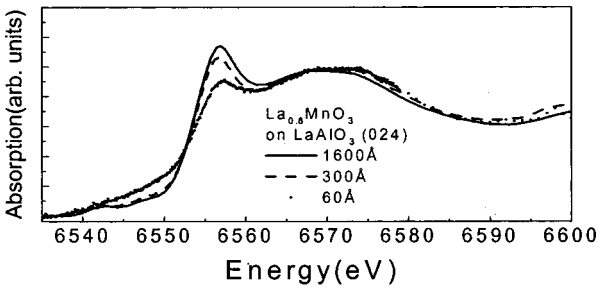

FIG. 3. Near-edge x-ray absorption spectra (Mn *K*) of $La_{0.8}MnO_3$ films for 1600 Å (solid line), 300 Å (dashed line) and 60 Å (solid dot) films. The spectrum measured when the incident x-ray E-vector at 45° to film surface. Note the broad main line in the 60 Å film.

Local structural information can be gleaned from x-ray absorption measurements. We measured Mn *K*-edge absorption spectra of these films (Fig. 3). This spectrum shows a strong dependence of width of the 1*s* to "4*p*" peaks with thickness. The broadest and most narrow ones correspond to the 60 Å and 1600 Å films, respectively. We note that the 300 and 1600 Å have similar profiles while the 60 Å film is distinctly broader. In our recently work,[18,19] we have shown that in the manganites, the local distortions of the MnO_6 octahedra are manifested by the enhancement of the width of the main line.

The important point is that the 60 Å film has very large local distortions which are significantly larger than those present in stoichiometric $LaMnO_3$ (see Refs. 18 and 19). Yet, this film is ferromagnetic and metallic. This indicates that the film is mainly composed of a strained layer with a covering metallic B layer. The two layer growth has been seen by others.[2,20] However, here we addressed the evolution of the relative A and B volumes with thickness on multiple length scales.

Data acquisition was performed at NSLS in BNL which is funded by the U.S. Department of Energy grant DE-AC02-98CH100886. This work was supported by NSF Career Grant No. DMR-9733862 and by NSF/CNRS Project No. 9159.

[1] Y. Tokura and Y. Tomioka, J. Magn. Magn. Mater. **200**, 1 (1999), and references therein; J. M. Coey, M. Verit, and S. von Molenar, Adv. Phys. **48**, 167 (1999), and references therein.
[2] S. Jin, T. H. Tiefel, M. McCormack, H. M. O'Bryan, L. H. Chen, R. Ramesh, and D. Schurig, Appl. Phys. Lett. **67**, 557 (1995).
[3] M. G. Blamire, B.-S. Teo, J. H. Durrell, N. D. Mathur, Z. H. Barber, J. L. McManus Driscoll, L. F. Cohen, and J. E. Evetts, J. Magn. Magn. Mater. **191**, 359 (1999).
[4] J. Z. Sun, D. W. Abraham, R. A. Rao, and C. B. Eom, Appl. Phys. Lett. **74**, 3017 (1999).
[5] Y. Suzuki, H. Y. Hwang, S. W. Cheong, and R. B. van Dover, Appl. Phys. Lett. **71**, 140 (1997).
[6] X. W. Wu, M. S. Rzchowski, H. S. Wang, and Q. Li, Phys. Rev. B **61**, 501 (2000).
[7] H. S. Wang, Q. Li, K. Liu, and C. L. Chien, Appl. Phys. Lett. **74**, 2212 (1999); H. S. Wang and Q. Li, *ibid.* **73**, 2360 (1998).
[8] T. K. Nath, R. A. Rao, D. Lavric, C. B. Eom, L. Wu, and F. Tsui, Appl. Phys. Lett. **74**, 1615 (1999).
[9] J. O'Donnell, M. S. Rzchowski, J. N. Eckstein, and I. Bozovic, Appl. Phys. Lett. **72**, 1775 (1998).
[10] A. J. Millis, T. Darling, and A. Migliori, J. Appl. Phys. **83**, 1588 (1998).
[11] A. J. Millis, A. Goya, M. Rajeswari, K. Ghosh, R. Shreekala, R. L. Greene, R. Ramesh, and T. Venaatesan (unpublished).
[12] Z. Fang, I. V. Solovyev, and K. Terakura, Phys. Rev. Lett. **84**, 3169 (2000).
[13] J. Aarts, S. Freisem, R. Hendrikx, and H. W. Zandbergen, Appl. Phys. Lett. **72**, 2975 (1998).
[14] H. L. Ju, Kannan M. Krishnan, and D. Lederman, J. Appl. Phys. **83**, 7073 (1998).
[15] S. Pignard, H. Vincent, J. P. Sénateur, and J. Pierre, J. Magn. Magn. Mater. **177**, 1227 (1998).
[16] J. P. Sénateur, R. Madar, F. Weiss, O. Thomas, A. Abrutis, French Patent No. 2,707,671 (1993), European Patent No. 730,671 (1994), US Patent No. 5,945,162 (1999).
[17] F. Felten, J. P. Senateur, F. Weiss, R. Madar, and A. Abrutis, J. Phys. IV **5**, 1079 (1995); C. Dubourdieu, M. Audier, J. P. Sénateur, and J. Pierre, J. Appl. Phys. **86**, 6945 (1999).
[18] Q. Qian, T. A. Tyson, C.-C. Kao, W. Prellier, J. Bai, A. Biswas, and R. L. Greene, Phys. Rev. B **63**, 224424 (2001).
[19] Q. Qian, T. A. Tyson, C.-C. Kao, M. Croft, S.-W. Cheong, G. Popov, and M. Greenblatt, Phys. Rev. B **64**, 024430 (2001).
[20] W. Prellier, A. Biswas, M. Rajeswari, T. Venkatesan, and R. L. Greene, Appl. Phys. Lett. **75**, 397 (1999); A. Biswas, M. Rajeswari, R. C. Srivastava, Y. H. Li, T. Venkatesan, R. L. Greene, and A. J. Millis, Phys. Rev. B **61**, 9665 (2000).